Cell and Tissue Research (2021) 386:261–280
https://doi.org/10.1007/s00441-021-03503-x

REGULAR ARTICLE

The mRNA decapping protein 2 (DCP2) is a major regulator of developmental events in *Drosophila*—insights from expression paradigms

Rohit Kunar[1] · **Jagat Kumar Roy**[1]

Received: 24 January 2020 / Accepted: 1 July 2021 / Published online: 18 September 2021

Abstract
The *Drosophila* genome codes for two decapping proteins, DCP1 and DCP2, out of which DCP2 is the active decapping enzyme. The present endeavour explores the endogenous promoter firing, transcript and protein expression of *DCP2* in *Drosophila* wherein, besides a ubiquitous expression across development, we identify an active expression paradigm during dorsal closure and a plausible moonlighting expression in the Corazonin neurons of the larval brain. We also demonstrate that the ablation of *DCP2* leads to embryonic lethality and defects in vital morphogenetic processes whereas a knockdown of *DCP2* in the Corazonin neurons reduces the sensitivity to ethanol in adults, thereby ascribing novel regulatory roles to DCP2. Our findings unravel novel putative roles for DCP2 and identify it as a candidate for studies on the regulated interplay of essential molecules during early development in *Drosophila*, nay the living world.

Keywords Corazonin · DCP2 · *Drosophila* development · Epithelial morphogenesis · Ethanol sedation

Introduction

Organismal development mimics an orchestra with precisely timed and fine-tuned role(s) for each of the players. Balanced expression of genes requires timed activity of gene promoters at the proper site along with orderly degradation of transcripts and/or proteins (Yao and Ndoja 2012; Ding 2015). Decay of transcripts is one of the strategies to regulate gene expression (Ghosh and Jacobson 2010), and the mRNA decapping proteins (DCPs) assume prime importance therein. These proteins initiate degradation of the mRNAs in cytoplasmic foci known as P-bodies, by removal of the 7-methylguanosine cap at the 5′ end of the mRNAs (Coller and Parker 2004). The *Drosophila* genome codes for two mRNA decapping proteins, *viz*., DCP1 and DCP2, out of which DCP2 is the active decapping enzyme. While DCP1 functions to activate DCP2 (Ren et al. 2012) and P-bodies/DCP1 have been implicated in miRNA-mediated gene silencing (Rehwinkel et al. 2005), localization of the oskar mRNA in the *Drosophila* oocyte (Lin et al. 2006) and in oogenesis (Lin et al. 2008), DCP2 has been implicated in chronic nicotine–induced locomotor hyperactivity in *Drosophila* (Ren et al. 2012). However, characterization of the role of decapping proteins in development has been limited to *Arabidopsis* (Xu et al. 2006) and *Caenorhabditis elegans* (Lall et al. 2005) only. Despite being the primary decapping protein in *Drosophila*, the spatio-temporal dynamics of *DCP2* activity remain unexplored. The *DCP2* gene in *Drosophila* is ~ 8 kb in length and has two curated promoters, *viz*., a proximal promoter DCP2_1 and a second, downstream promoter DCP2_2 (Eukaryotic Promoter Database, EPD; Dreos et al. 2014) and codes for four transcripts (FlyBase; Drysdale 2008). Herein, we have tried to explore the temporal activity of the *DCP2* promoter using the conventional *UAS-GAL4* system (Brand and Perrimon 1993) wherein we used a GAL4 driven by the *DCP2* promoter ($DCP2^{GAL4}$; Lukacsovich et al. 2001; Ren et al. 2012) and combined it with a modified UAS line (G-TRACE; Evans et al. 2009) to delineate the real-time promoter activity of *DCP2* during embryonic dorsal closure and in the larval tissues. In parallel, we endeavoured to delineate the expression

✉ Jagat Kumar Roy
jkroy@bhu.ac.in

Rohit Kunar
rohit.kunar3@bhu.ac.in

[1] Cytogenetics Laboratory, Department of Zoology, Institute of Science, Banaras Hindu University, Uttar Pradesh, Varanasi 221005, India

of the transcript isoforms or splice variants generated and the expression paradigm of the translated protein. Although *DCP2* is highly active and ubiquitous, a selectively elevated expression of the DCP2 protein was observed in the Corazonin (Crz) neurons of the larval brain and renders the individuals less sensitive to ethanol when knocked down in the corazonin neurons, while in the larval wing pouch, DCP2 is expressed along the A-P and D-V axes. *Loss-of-function* mutants of *DCP2* are embryonic lethal and showed defects in epithelial morphogenesis and organization of the embryonic nervous systems along with elevation and spatial disruption of the JNK cascade. Collectively, our observations identify DCP2 as a potential candidate for explication of molecular interplay during *Drosophila* development.

Materials and methods

Fly strains, genetics and lethality assay

All flies were raised on standard agar-cornmeal medium at 24 ± 1 ºC. *Oregon* R^+ was used as the wild-type control. For targeted gene expression (Brand and Perrimon 1993), $DCP2^{BG01766}/TM3$, Ser^1 ($DCP2^{GAL4}$; Ren et al. 2012), *CCAP-GAL4*, *TH-GAL4*, *Ap-GAL4*, *Ddc-GAL4*, *UAS-GFP*, *UAS-mCD8::GFP* and $UAS\text{-}DCP2^{RNAi}$ were obtained from the Bloomington *Drosophila* Stock Centre, while G-TRACE/CyO (Evans et al. 2009) was a kind gift from Prof. Utpal Banerjee, MBI, UCLA. $DCP2^{e00034}/TM3$, Ser^1 was obtained from the Harvard *Drosophila* Stock Centre. The JNK signalling bio-sensor, *TRE-RFP* (Chatterjee and Bohmann 2012; referred to as *TRE-JNK* in the text), was obtained as a kind gift from Prof. B. J. Rao, TIFR, Mumbai, India, while *sNPF-GAL4*, *Dilp2-GAL4* and *Crz-GAL4/CyO* were obtained from Prof. Gaiti Hasan, NCBS, Bangalore, India.

$DCP2^{BG01766}/TM3$, Ser^1 and $DCP2^{e00034}/TM3$, Ser^1 were further introgressed with *TM3*, *ActGFP*, $Ser^1/TM6B$ stock in order to generate $DCP2^{BG01766}/TM3$, *ActGFP*, Ser^1 or $DCP2^{e00034}/TM3$, *ActGFP*, Ser^1 stocks. *TRE-JNK* (Chatterjee and Bohmann 2012) was introgressed with *Sp/CyO*; $DCP2^{BG01766}/TM3$, *ActGFP*, Ser^1 or *Sp/CyO*; $DCP2^{e00034}/TM3$, *ActGFP*, Ser^1 to obtain *TRE-JNK*; $DCP2^{BG01766}/TM3$, *ActGFP*, Ser^1 or *TRE-JNK*; $DCP2^{e00034}/TM3$, *ActGFP*, Ser^1 stocks, respectively.

For behaviour assays, *Crz-Gal4/CyO* flies were crossed to w^{1118} or $UAS\text{-}DCP2^{RNAi}$ flies to generate *Crz-Gal4/+* (Control) or *Crz-Gal4/+*; $UAS\text{-}DCP2^{RNAi}/+$ (experimental) genotypes.

Embryonic lethality was calculated as described in Bhuin and Roy (2009). One hundred embryos were transferred to agar plates and incubated for 24 to 48 h at 23°C, and the total number of dead embryos was counted against the total number of fertilized eggs. These fertilized eggs include the dead as well as the hatched embryos. The percentage of lethality was calculated as.

(No. of dead embryos/No. of fertilized embryos) × 100%

The percentage (%) lethality for each cross was calculated in triplicates, and the mean lethality so obtained was tabulated and graphically represented using MS Excel 2010. The final percentages have been calculated by multiplying the lethality obtained in every cross scheme with the inverse of the fraction of the progeny determined by standard Mendelian ratios.

Detection of DCP2 transcript expression and analysis of splice variants

Detection of transcript expression from *DCP2* was performed by reverse-transcriptase polymerase chain reaction (RT-PCR) using a combination of primers designed such that the amplicon size would discriminate between the individual isoforms which included a single reverse primer, DCP2_DBAE_R, which could bind to all of the transcripts, and two forward primers, *viz*., DCP2_BAE_F, which would bind to isoforms DCP2-RA, RB and RE, and DCP2_D_F, which would bind to DCP2-RD. Being similar in architecture, DCP2-RA and RE would yield similar-sized amplicons with the above primer pair, but DCP2-RD would yield a smaller amplicon. However, the 3′UTR is longer and unique for DCP2-RE, and this architectural bias was exploited to discriminate between the two isoforms by designing an additional primer pair which would amplify the 3′UTR sequence of DCP2-RE uniquely. Table 1 shows the primer sequences, the combinations and the calculated amplicon sizes for each

Table 1 List of primer sequences, combinations generated and calculated amplicon sizes for detection of expression of *DCP2* transcript isoforms

Primer Pair	Sequence (5′-3′)	Amplicon size(in base pair)			
		RD	RB	RA	RE
DCP2_D_F DCP2_DBAE_R	ACAACGATTCAATACATATACAGCT CTGTTTTTGTTGCTCGTGTTGT	***165***	–	–	–
DCP2_BAE_F DCP2_DBAE_R	GCAATTTAGATCGCGAAAAAGTTC CTGTTTTTGTTGCTCGTGTTGT	–	***159***	***974***	974
DCP2_EU_F DCP2_EU_R	TCATTTGTCTGGGCCAAGTGAC TGGGATTGCAGTTCATCAAATG	–	–	–	***233***

of the isoform with each of the primer pairs. The unique amplicons are italicized. RT-PCR was performed according to Lakhotia et al. (2012) in the samples discussed in the "Results and discussion" section.

Embryo collection and fixation

All flies were made to lay eggs on standard agar plates supplemented with sugar and propanoic acid and eggs were collected according to Narasimha and Brown (2006), with slight modifications. For whole mount preparations and immunostaining of embryos, different alleles and transgenes were balanced with GFP tagged balancers, and only non-GFP or driven embryos were selected for experimental purpose. Embryo staging was done according to Hartenstein's Atlas of *Drosophila* Development (1993).

Immunocytochemistry

Drosophila embryos were fixed and imaged as described by Narasimha and Brown (2006). The dechorionated and devitellized embryos were fixed in 4% para-formaldehyde solution and stored in absolute methanol. Immunostaining of the embryos was done as described in Nandy and Roy (2020). Late third instar larval tissues were dissected out in 1 × PBS, fixed in 4% paraformaldehyde for 20 min at RT and immunostained as described previously in Banerjee and Roy (2017). The primary antibodies used were mouse anti-DCP2 (1:50; PCRP-DCP2-1D6, DSHB), mouse anti-Fasciclin II (1:100; 1D4, DSHB), mouse anti-Fasciclin III (1:100; 7G10, DSHB) and rabbit anti-phospho-JNK/SAPK (1:100; 81E11 Cell Signaling Technology). Appropriate secondary antibodies conjugated either with Cy3 (1:200, Sigma-Aldrich, India) or Alexa Fluor 488 (1:200; Molecular Probes, USA) or Alexa Fluor 546 (1:200; Molecular Probes, USA) were used to detect the given primary antibody, while chromatin was visualized with DAPI (4′, 6-diamidino-2-phenylindole dihydrochloride, 1 µg/ml Sigma-Aldrich). For imaging of live embryos for real-time promoter analysis using G-TRACE or for JNK signalling using TRE-JNK, embryos of the desired genotype were rinsed in 1X PBS, dechorionated in bleach and mounted in halocarbon oil and observed directly.

Cuticular preparations from embryos

Cuticle preparations were made from embryos as described by Wieschaus and Nusslein-Volhard (1986) along with some modifications as described in Sasikumar and Roy (2009). Briefly, the eggs were dechorionated in bleach and washed in an aqueous solution containing 0.7% NaCl and 0.02% Triton-X 100. The eggs were washed thrice in 0.1% Triton-X, devitellinised in a mixture of methanol and *n*-heptane (1:1 v/v). They were fixed in 1 part glycerol, 4 parts acetic acid for 1 h, mounted in Hoyer's mountant and cleared at 60ºC overnight.

Microscopy and documentation

The immunostained slides were observed under Zeiss LSM 510 Meta Laser Scanning Confocal microscope, analysed with ZEN12 and LSM software and assembled using Adobe Photoshop 7.0. The cuticles were observed in dark field or phase-contrast optics, namely 10X Plan Fluor Ph1 DLL (0.3 NA), 20X Plan Fluor Ph1 DLL (0.5 NA) and 40X Plan Fluor Ph2 DLL (0.75 NA) objectives (Nikon, Japan), and images were captured with a Nikon Digital camera DXM1200. Fluorescence imaging of embryos for analysis of *DCP2* promoter using G-TRACE or JNK signalling was done in Nikon 90i Fluorescence microscope under 10X Plan Fluor Ph1 DLL (0.3 NA), 20X Plan Fluor Ph1 DLL (0.5 NA) objectives.

Behaviour assay

Groups of 20 males or females (1–3 days old) of the desired genotypes, *viz*., *Crz-Gal4/+* (Control) and *Crz-Gal4/+*; $UAS\text{-}DCP2^{RNAi}/+$ (Experimental), maintained on food vials in a 12L/12D conditions at 23ºC for 1 day, were used for the following behaviour assays.

Ethanol sedation assay

Ethanol sedation assays were performed as described previously (McClure and Heberlein 2013) with minor alterations. Briefly, flies were transferred to empty vials, sealed with cotton plugs and allowed to acclimatize for 10–20 min. The cotton plugs were replaced with fresh plugs containing 1 ml of 100% ethanol. They were maintained in such "booze chambers" for 15–20 min. During the treatment, flies were mechanically stimulated by tapping and/or mechanically swirling the vials at intervals of 5 min. Flies able to climb the walls and/or move their appendages on the floor of the vial were considered "non-sedated" while those unable to execute such activity were considered "sedated". The number of sedated flies was counted at 5 min intervals. The time to 50% sedation (ST50) was determined by manual intrapolation.

Recovery from ethanol sedation

Recovery from ethanol induced sedation was assayed as described by Sha et al. (2014). Following exposure to ethanol (described above), the cotton plugs were replaced with fresh plugs, and the vials were inverted to place them upside down. The number of "non-sedated" flies (considered as "recovered") was counted every 10 min.

Results and discussion

DCP2 mRNAs are expressed ubiquitously throughout *Drosophila* development

In order to determine the presence or absence of DCP2 transcripts at a particular stage along with identification of the exact isoform(s)/splice variant(s) expressed therein, RT-PCR was performed using primers designed for the same. DCP2 expression was detectable at all stages of development, *viz*., embryonic (0-24 h), larval (1st, 2nd and 3rd instars), pupal and adult stages. Among the four annotated variants, DCP2_RE (FBtr0304975) (Fig. 1d, h) and DCP2_RA (FBtr0075538) (Fig. 1a, e) were observed in all stages of fly development, whereas DCP2_RD (FBtr0100528) was observed only in the larval gonads, *viz*., testes and ovaries, and in the adult fly body (Fig. 1c, g). The other variant, DCP2_RB (FBtr0075539), was detectable only in the pupae and adults but was absent in larval stages (Fig. 1b, f). Out of the four isoforms however, DCP2_RA and DCP2_RE are observed to be expressed throughout development, but DCP2_RE appears to be the most abundant and ubiquitous isoform expressed. Although DCP2-RB is driven by the same promoter which drives DCP2_RA and RE, its absence does not necessarily indicate dearth of expression. In silico analyses and data mining from the Eukaryotic Promoter Database (Dreos et al. 2014, 2017) indicate that DCP2-RD may be driven by the second promoter of DCP2 (DCP2_2). The protein isoforms coded by DCP2_RB and DCP2_RD are identical in sequence and size, but the exclusive expression of DCP2_RD in the larval gonadal tissues (ovaries and testes) and at a very low titre in the adults plausibly owing to the promoter being responsive to transcription factors in the gonadal tissues only and/or a putative undiscovered function of the transcript therein, despite absence of visible quantities of DCP2_RB.

DCP2 expresses in cells of diverse developmental lineages in the *Drosophila* embryo and the *DCP2* promoter *vis-à-vis DCP2* is active since early development

Evolution has been parsimonious in designing genes and ascribing roles to them, and hence, determination of gene functions becomes incomplete without identification of the expression dynamics of the gene. In order to determine the endogenous expression pattern of *DCP2* in *Drosophila melanogaster*, we used the $DCP2^{GAL4}$ ($DCP2^{BG01766}$) which has a P{GT1}construct (Lukacsovich et al. 2001) bearing a GAL4, immediately downstream to the *DCP2* promoter. Using GFP as a reporter, we detected extremely robust signal in the late embryonic stages, wherein it expresses strongly in the embryonic epithelia (ectoderm) (Fig. 2a), the central nervous system (neuro-ectoderm) (Fig. 2b) and the dorsal muscles (mesoderm) (Fig. 2c) and is uniformly ubiquitous in all the segments in the embryo. With such a robust expression (of GFP), which is actually driven by the *DCP2* promoter, it is evident that *DCP2* is expressed and is active in embryonic cells derived from differing developmental lineages.

Dorsal closure is a major morphogenetic event during embryonic development in *Drosophila* (Martinez-Arias 1993) and involves an orchestrated interplay of numerous molecules (Lada et al. 2012) to drive the concerted movement of lateral epithelial cell sheets. With *DCP2* being expressed strongly in the embryonic epithelium, we investigated the possibility and nature of activity of the *DCP2* promoter during dorsal closure. To determine the real-time activity of the *DCP2* promoter during dorsal closure, we used a GAL4-responsive tripartite construct, G-TRACE (Evans et al. 2009). Using this transgenic line, in the embryonic stages (Fig. 3), we observed that *DCP2* expresses in a more or less ubiquitous pattern very early in development, even prior to stage 10 (Fig. 3a). However, real-time expression was not detected in stage 10, in which the germband is fully extended (Fig. 3b, d), and stage 12, wherein the germband is

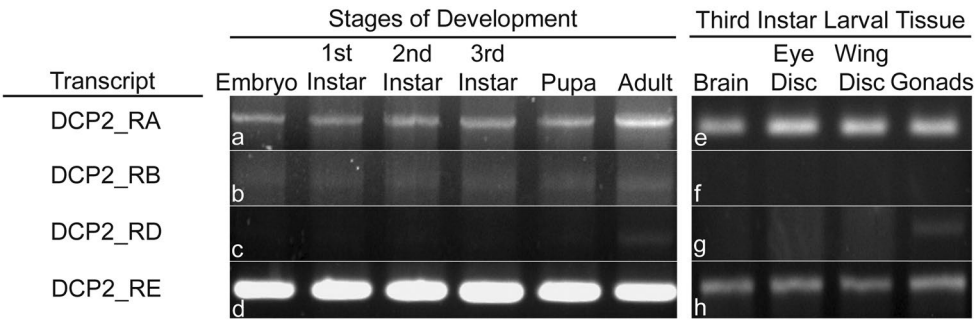

Fig. 1 Electrophoretogram showing the expression pattern of different isoforms or splice variants of *DCP2* across *Drosophila* development (**a**–**d**) and in selected third instar larval tissues (**e**–**h**)

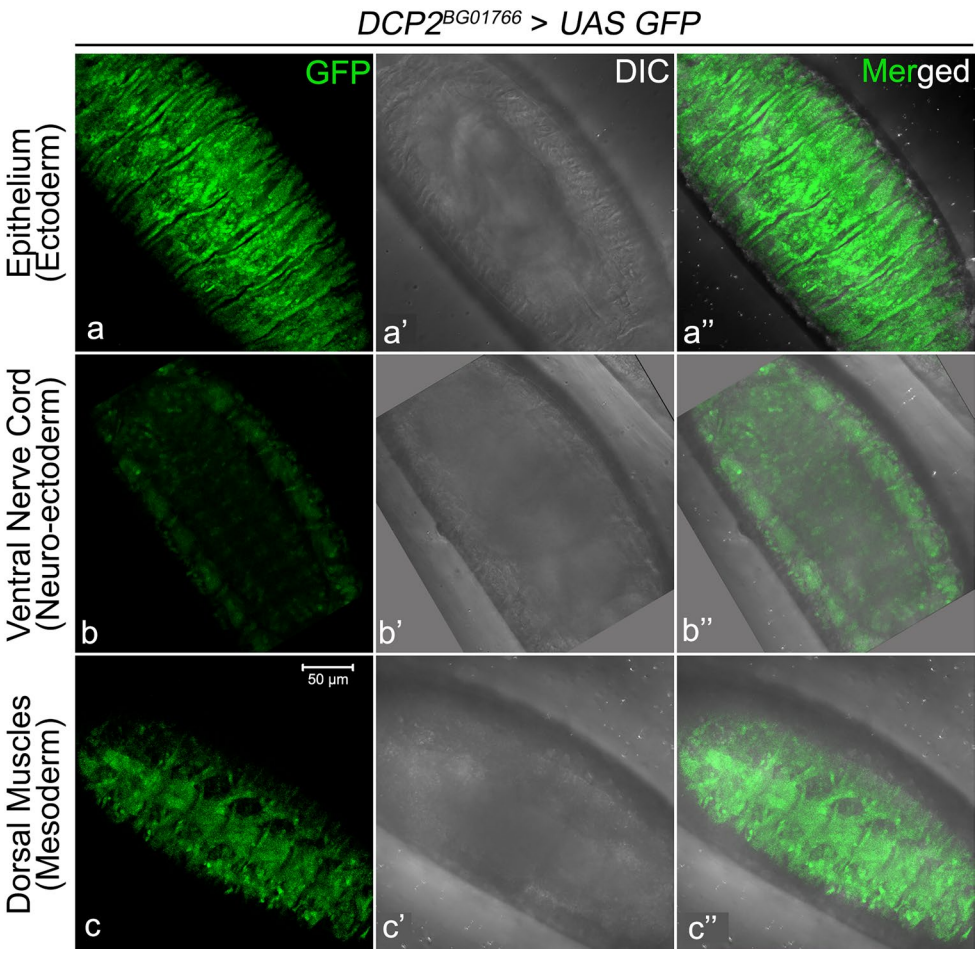

Fig. 2 Confocal projections of late embryos (stage 17) showing endogenous expression pattern of *DCP2* as determined by expression of GFP (green) by $DCP2^{GAL4}$. Tissues of differing developmental lineages, *viz*., ectoderm (**a**-**a″**), neuroectoderm (**b**-**b″**) and mesoderm (**c**–**c″**) show robust expression of GFP. Scale bar shows 50 µm

fully retracted (Fig. 3j, l). In the intervening stage, wherein the germband starts retracting, *i.e*., stage 11, we detect strong expression of *DCP2* (Fig. 3f, h). Again, when the epithelial sweeping initiates following germband retraction (stage 13), we see a surge in the RFP expression (Fig. 3n, p) which intensifies further in stage 14, in which the lateral epithelia on either side are still moving (Fig. 3r, t). This intense RFP expression is visible in stage 16 as well (Fig. 3v, x). The stages 10 and 12 are developmental periods of low cell migration as against stages 11, 13 and 14 wherein the epithelium moves as an initiative of collective cell migration and coordinated cell-shape changes. The expression potential of the *DCP2* promoter across DC revealed expression "crests and troughs", such that the "crests" paralleled the periods in which cellular mobility or migration was maximal and *vice versa* (Fig. 3y). The RFP activity is detectable only in stages which involve collective cell movement. The eGFP expression however depicts an early initial pulse of the gene expression which plausibly maintains a basal level of gene product. Hence, the dynamics of the promoter reflects a tightly regulated expression of *DCP2* and brings to light that *DCP2* may be an essential player during collective cell migration *vis-à-vis* epithelial morphogenesis.

DCP2 expresses in the amnioserosa and lateral epithelium during dorsal closure and its loss affects survival, epithelial morphogenesis and development of nervous system in the *Drosophila* embryo

During the later stages of dorsal closure, parallel to the contralateral movement of the epithelia towards the dorsal side, the axon pathways are established in the CNS across the ventral nerve cord, which form the complete nervous system by the end of stage 16 (Bhuin and Roy 2009). Since *DCP2* shows active expression paradigms during embryonic dorsal closure (Fig. 3), we examined the expression of DCP2 in the lateral epithelia in stage 13 embryos along with the expression of activated JNK, a key mediator of dorsal closure (Jacinto et al. 2002), and Fasciclin III, a cell adhesion molecule (Bahri et al. 2010), both of which are expressed at the lateral epithelia and the leading edge (LE) cells. DCP2 was found to be expressed in the amnioserosa and throughout the lateral epithelium as well as in the cells at the LE (Fig. 4). Examination of the ventral nerve cord also showed strong cytoplasmic expression of DCP2 (Fig. 5).

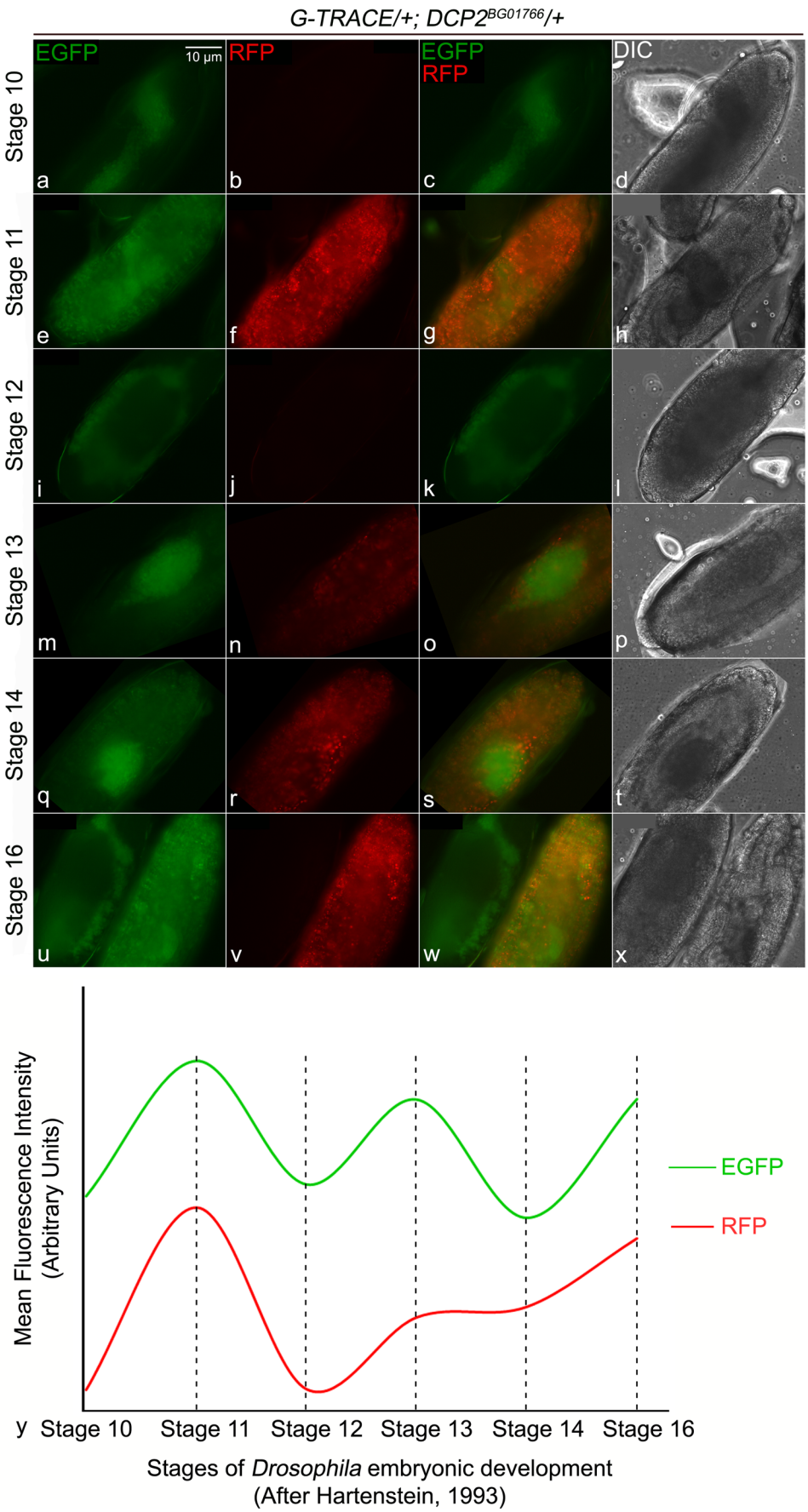

Fig. 3 Lineage specific (EGFP) and real time (RFP) expression of *DCP2* in the embryonic stages using the GAL4-UAS based G-TRACE system. **a**–**x** show the expression pattern of the reporters along with the DIC images of the embryos. While real-time *DCP2* promoter activity is not detectable during stages 10 and 12 and is low in stage 13, it is robust in stages 11 and 14. y shows a plot of the fluorescence of both the reporters (GFP and RFP) across the stages observed, wherein a near-sinusoidal curve is obtained showing crests and troughs of *DCP2* promoter activity across the stages of Dorsal closure. Scale bar shows 10 µm

We found that embryos homozygous for loss-of-function alleles of *DCP2* (*viz*., $DCP2^{BG01766}$ and $DCP2^{e00034}$) show embryonic lethality. $DCP2^{BG01766}$ homozygotes are 100% embryonic lethal ($N=500$) whereas $DCP2^{e00034}$ homozygotes show 12% lethality ($N=500$) at the embryonic stage and the remaining die before reaching the second instar larval stage.

- **Defects in epithelial morphogenesis**

Since we found strong expression of *DCP2* in the embryonic epithelium, we endeavoured to explore whether a loss of *DCP2* function affects epithelial morphogenesis. Analysis of embryonic cuticles showed that all mutants displayed pronounced defects in epithelial morphogenesis patterns, ranging from defects in size, *viz*., anterioposterior or dorsoventral dimensions, head involution defects and morphological defects, *viz*., u-shaped or puckering (Fig. 6). Since these defects are not mutually exclusive in that a single-mutant embryo could be displaying multiple defects at the same time, the morphological aberrations were scored individually first and then analysed for the presence of other concomitant defects. While 82.6% of the $DCP2^{BG01766}$ homozygotes ($N=120$) show altered anterioposterior or dorsoventral dimensions (*viz*., elongated or compressed) of which 68.4% embryos are defective in head involution and 36.8% embryos are puckered, 21.7% embryos have gross defects in all the morphological parameters analysed. A total of 4.3% of the embryos are exclusively puckered, and 6.5% embryos show defects in head involution only. None of the $DCP2^{e00034}$ homozygotes ($N=100$) analysed was exclusively puckered. Eighty per cent of the embryos observed show altered dimensions out of which 12.5% are puckered and are defective in head involution, and 62.5% embryos are not puckered but show head involution defects. Twenty per cent of the embryos observed show defects exclusively in dimensions or head involution. Figure 7 shows the above data represented with the help of a Venn diagram along with the lethality at the embryonic stage.

- **Defects in nervous system development**

We used mAbBP102, an antibody to mark all CNS axons (Seeger et al. 1993) such that the gross morphology of CNS in an embryo is revealed. In wild-type embryos, axons form an orthogonal structure having longitudinal axon tracts. These axon tracts run anterioposteriorly, being positioned at either side of the midline, and a pair of commissural tracts joins the longitudinal pathways in each segment of the embryo (Bhuin and Roy 2009). $DCP2^{BG01766}$ homozygotes showed thinning of longitudinal connectives and compressed segmental commissures (Fig. 8b, b′) similar to the *karussell* phenotype (Hummel et al. 1999), whereas $DCP2^{e00034}$ homozygotes showed thinning of longitudinal connectives and lateral commissures (Fig. 8c, c′). In order to study the embryonic PNS axons further, mutant embryos were stained with mAb22C10, which recognizes the microtubule-associated protein, futsch (Hummel et al. 2000). It labels all the cell bodies, dendrites and axons of all PNS neurons, and a subset of neurons in the VNC of the CNS (Fujita et al. 1982). Therefore, defects, such as the disruption of the nervous system, the collapse of the axon tracts, fasciculation defects/thinning of axons and the loss or gain of neurons, can often be distinguished. In the wild-type embryos, each segment contains three highly stereotyped clusters of PNS neurons connected by axon bundles. In the mutants, misrouting of axons and collapsed axons could be detected (Fig. 8e, e′, f, f′), which were absent in the wild type, implying a role for DCP2 in the fasciculating axons.

In the developing *Drosophila* embryo undergoing gastrulation, epithelial morphogenesis and axonogenesis are morphogenetic events of utmost importance that require a well-orchestrated spatiotemporal regulation of gene expression. During initiation of dorsal closure wherein the two lateral epithelia initiate contralateral movement to eventually seal the dorsal opening, the dorsal-most lateral epithelial cells express high levels of JNK (Noselli and Agnes 1999). The JNK signalling pathway is a core signalling pathway in the process of dorsal closure at the time of gastrulation in *Drosophila* embryos (Noselli 1998; Noselli and Agnes 1999; Ramet et al. 2002; Stronach and Perimon 2002).While DCP2 co-expresses with JNK ubiquitously on the dorsolateral epithelia, the leading edge and the amnioserosa, monitoring the activity of the *DCP2* promoter in real time across the stages of dorsal closure, show spurts of promoter firing in the stages which involve large-scale cell migration and movement. Such subtle and precisely timed gene activity is indicative of thorough fine-tuning of the expression of *DCP2*. The ablation of *DCP2* does not lead to "dorsal open" embryos but generates a spectrum of defects including altered embryonic dimensions and defects in head involution, improper fasciculation of axons and defects in segmental commissures and longitudinal connectives; causes embryonic and larval lethality implying significant perturbation in these developmental gene expression programs and indicates a more concerted and fundamental role of *DCP2* in regulating these phenomena. It is worth mentioning that despite ubiquitous expression of *DCP2*, the ectodermal (epithelium) and neuro-ectodermal (CNS and PNS) tissues are most affected following ablation. It is interesting to note that while the nematode worm is a closer relative of the fly in the evolutionary tree, the embryonic lethality and the developmental defects are similar to those observed in a distant relative, *Arabidopsis* wherein the loss of *DCP2* leads to seedling lethality (Xu et al. 2006; Goeres et al. 2007). Further,

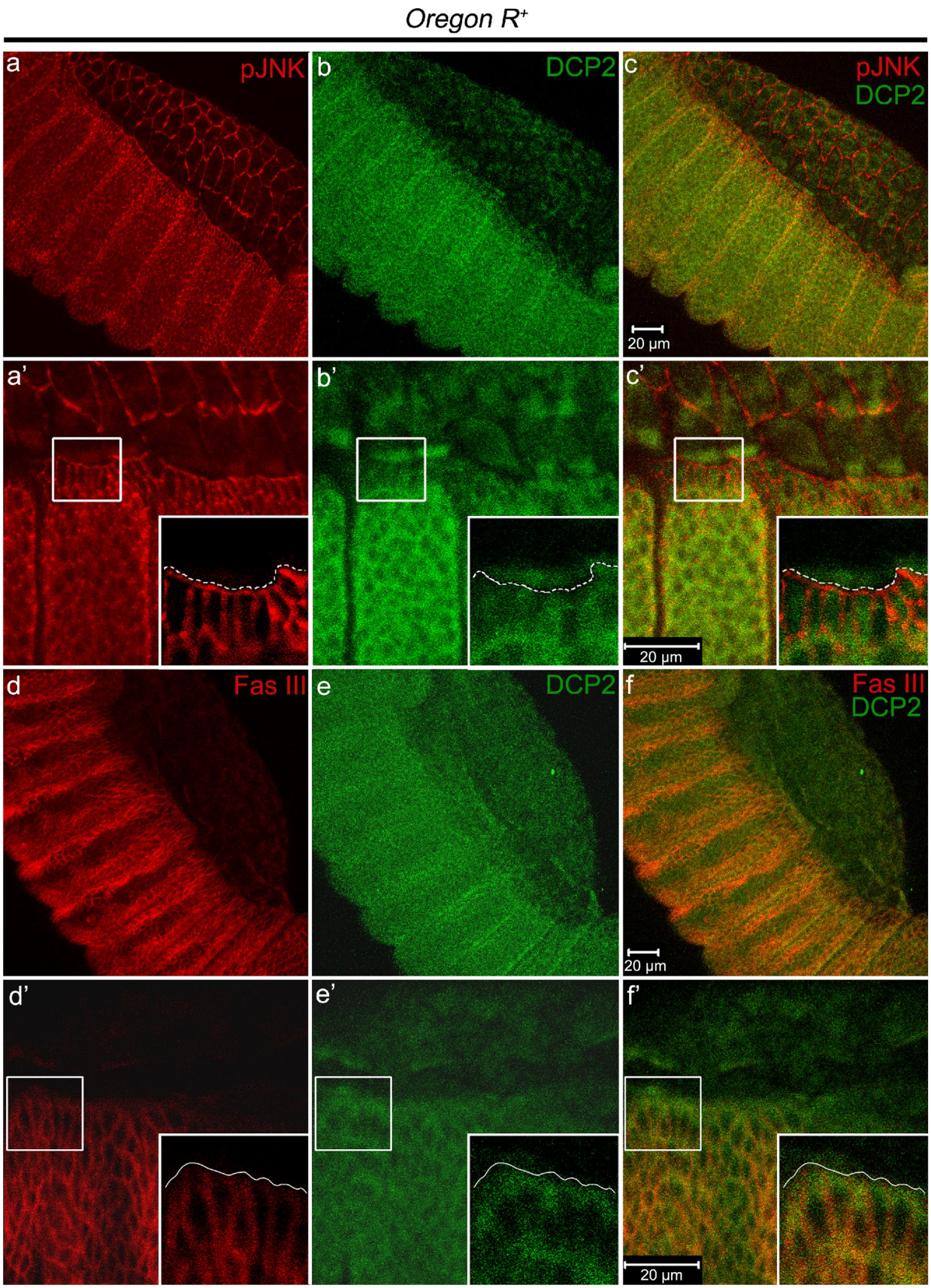
Oregon R+
a
pJNK
b
DCP2
c
pJNK
DCP2
20 µm
a'
b'
c'
20 µm
d
Fas III
e
DCP2
f
Fas III
DCP2
20 µm
d'
e'
f'
20 µm

◂**Fig. 4** Confocal projections showing immunolocalisation of DCP2 in the amnioserosa and the lateral epithelium in stage 13 embryos of wild type strain, co-stained for phospho-JNK (**a**–**c**) or the septate junction marker FasIII (**d**–**f**). In both cases, punctate expression of DCP2 in the lateral epithelium and amnioserosa (**b**, **e**) and at the leading edge (**b′** and **e′**) is clearly visible. Scale bars show 20 µm

both loss-of-function mutants of *DCP2*, *viz*., $DCP2^{BG01766}$ and $DCP2^{e00034}$ homozygotes, showed an elevation and spatial disruption of JNK signalling cascade, as evidenced by the JNK-biosensor (Supplementary Fig. 2). Since the JNK signalling pathway is fundamental to the process of dorsal closure during gastrulation in *Drosophila* embryos (Noselli 1998; Noselli and Agnes 1999; Ramet et al. 2002; Stronach and Perrimon 2002), and both epithelial morphogenesis and CNS development are dependent on JNK activity (Jacinto et al. 2002; Kushnir et al. 2017; Shklover et al. 2015; Karkali et al. 2020), the altered expression patterns of JNK or misdirected JNK signalling under the influence of loss of *DCP2* in the different alleles could be a probable cause of the defects observed in each case.

The *DCP2* promoter shows consistent developmental activity in the larval tissues along with tissue-specific expression paradigms of the translated protein

Real-time activity of the promoter in the various larval tissues, with a better insight, demonstrates that despite expression since early development, the *DCP2* promoter is active during late stages of larval development as well. In the larval tissues (118 ± 1 h ALH), we could identify a consistent GFP expression in the larval brain, eye-antennal disc, salivary gland and wing discs. Besides prior developmental activation and ubiquitous expression, the *DCP2* promoter shows enhanced activity/expression in specific cells in the brain (Fig. 9b, c) and eye disc (Fig. 9g, h), implying a consistent promoter activity during late larval development as well. Although, the ventral ganglion depicts an overlap of prior and real-time activity (Fig. 9b–d), the cerebral hemispheres show selective expression in real time, which is limited to cells of the antennal lobe and the Kenyon cells (Fig. 9b′-d′). Similarly, the cells in constituting the antennal disc show a more consistent *DCP2* activity, which exemplified the greater degree of overlap of the reporters (Fig. 9g-i). However, the cells of the eye disc show heterogeneity of reporter expression, *i.e.*, *DCP2* promoter is developmentally active in all the ommatidia, but certain cells show a transient or real activity at the stage observed (Fig. 9g′–i′). This demonstrates that the promoter is active in the tissue in the stage observed, similar to that observed in the other tissues. While the salivary gland nuclei show a complete colocalization of reporters with similar intensity (Fig. 9l–n), wing discs show a lower expression of eGFP as compared to RFP.

Since the GAL4 is driven by the de novo promoter of *DCP2*, which in absence of the GAL4 coding region would have transcribed the gene *per se*, this transgenic construct, *viz*., G-TRACE allows the spatio-temporal expression potential of the promoter to be determined. Thus, the expression of the reporters (eGFP and RFP) may be directly correlated with the gene expression pattern or potential in the wild-type individual and hence *via* the GAL4, directly demonstrating the spatiotemporal gene expression dynamics.

• Brain

In the larval brain, immunolocalisation of DCP2 shows a uniform cytoplasmic expression throughout the dorsoventral and anterioposterior axes of the tissue (Fig. 10a′, b′, d′). However, significantly high levels were detected in a subset of neurons in the ventral ganglion (Fig. 10a′, d′) and in a cluster of neurons in the dorsolateral and dorsomedial region of the central brain (Fig. 10a′, c′), which are proximal to the Mushroom Body as well as in the Kenyon cells (Fig. 10k, o). However, it is completely absent from the most prominent neuronal structures, *viz*., the Mushroom Body in the central brain and in the neurons of the optic lobe (Fig. 10m–o).

• Salivary glands

In the salivary glands, DCP2 shows a punctuate distribution in the cytoplasm and decorates the nuclear and cellular membranes arduously (Fig. 10e′, e″). The cytoplasmic vesicles appear bounded by bodies rich in DCP2 (Fig. 10e″). Since DCP2 is a cognate resident of the P-bodies, it may be fair enough to interpret the cytoplasmic network of DCP2 punctate in the glands as the pattern of P-bodies which are essential for maintaining transcript homoeostasis.

• Wing discs

The wing discs show very strong expression of DCP2 in the pouch region as compared with the notum (Fig. 10f′), besides the uniform ubiquitous cytoplasmic distribution similar to that observed in other tissues. Most notably, the expression of DCP2 in the central sections of the pouch overlaps with the expression of the anterioposterior determinant decapentaplegic (Dpp) (Zecca et al. 1995) and the dorsoventral determinant Wingless (Wg) (Neumann and Cohen 1997), thereby presenting a “cruciform” pattern in the pouch (Fig. 10g′), which may be essential during the morphogenesis of the wing blade.

Immunolocalisation of DCP2 to the cytoplasm in all the tissues examined across development recapitulates the

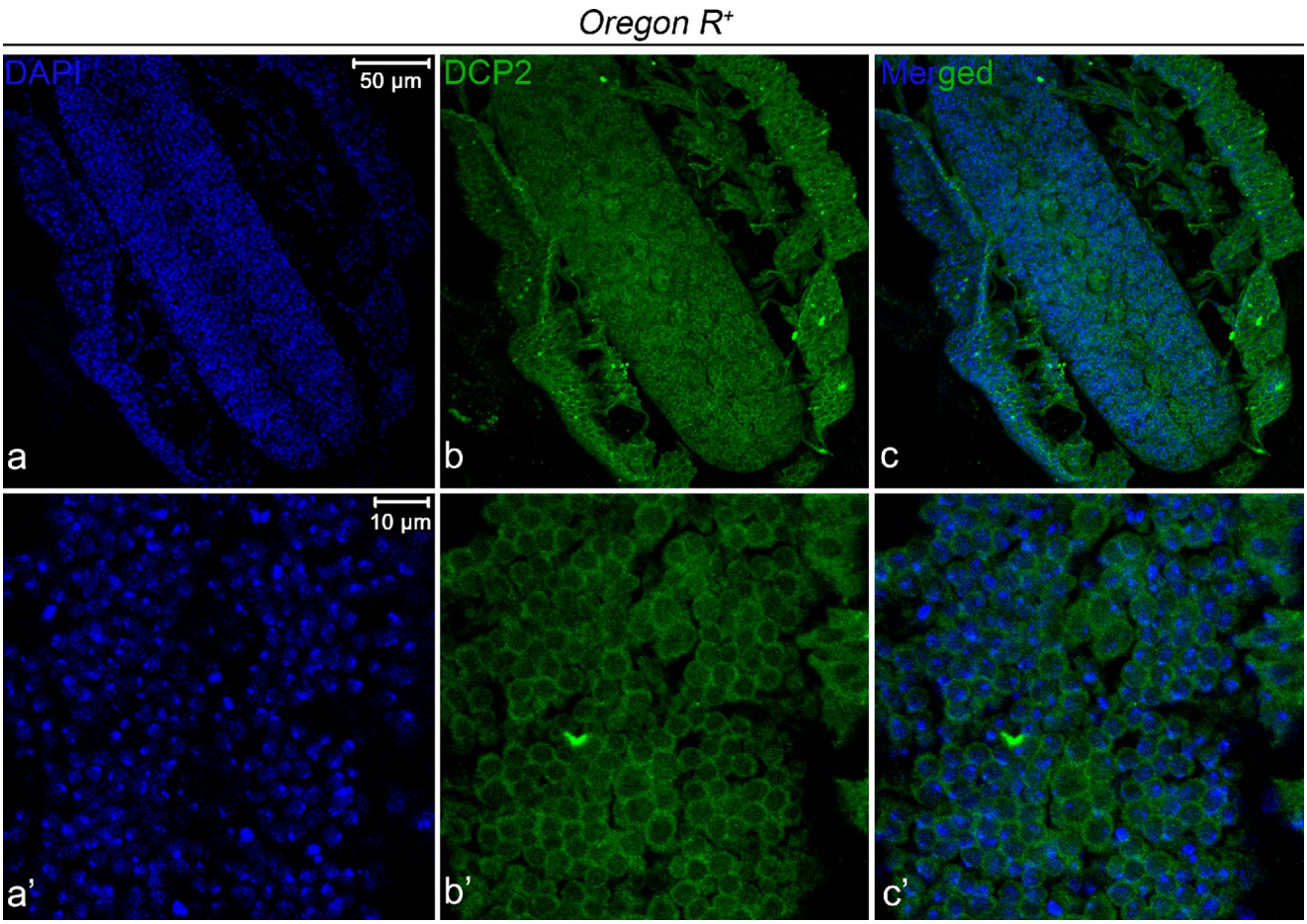

Fig. 5 Confocal projections showing immunolocalisation of DCP2 in the ventral nerve cord of stage 16 embryos of wild-type strain show cytoplasmic expression of DCP2 (**b**, **b′**) in the ventral nerve cord. Nuclei are counterstained with DAPI (**a** and **a′**). Scale bars show 50 µm (**a**–**c**) and 10 µm (**a′**–**c′**)

results observed in similar studies in the nematode worm, *C. elegans* (Lall et al. 2005), and in the thale cress, *Arabidopsis* (Xu et al. 2006). In spite of uniform ubiquitous cytoplasmic expression in the larval tissues, certain paradigms of expression have been noticed. The protein shows distinct punctate expression of the protein in the wing imaginal disc along the anterioposterior and dorsoventral axes in the wing pouch, mimicking the expression patterns of the TGF-beta homologue Decapentaplegic and Wingless, respectively. In the salivary glands as well, the protein is cytoplasmic but shows high titres at the membranes. Being the sole decapping agent in *Drosophila*, DCP2 is expressed ubiquitously throughout development but the selectively high expression in certain cell types in the brain or the wing pouch points towards some yet unknown "moonlighting" functions of *DCP2* in the development and maintenance of cellular homoeostasis in these tissues.

DCP2 shows high expression in the Corazonin neurons in the larval CNS

Besides ubiquitous expression, DCP2 has a typical expression paradigm in a subset of neurons in the larval CNS. In order to identify/type the DCP2 immunopositive neuron(s) in the larval ventral nerve cord (VNC), we tried mapping them against the Fasciclin II (FasII) landmark system (Santos et al. 2007) (Fig. 11). Comparing the FasII "coordinates" with the DCP2 expression paradigm, we observed that DCP2 expresses in a cluster of three neurons in the dorsolateral (DL) region and in a neuron located medial to the DL neurons (dorsomedial; DM) in the central brain, and in eight pairs of bilateral neurons in the ventral nerve cord. The neurons in the ventral ganglion correspond to a subset of the thoracic (T2 and T3) and abdominal (A1–A6) neuromeres. Although DCP2 is absent from the most prominent

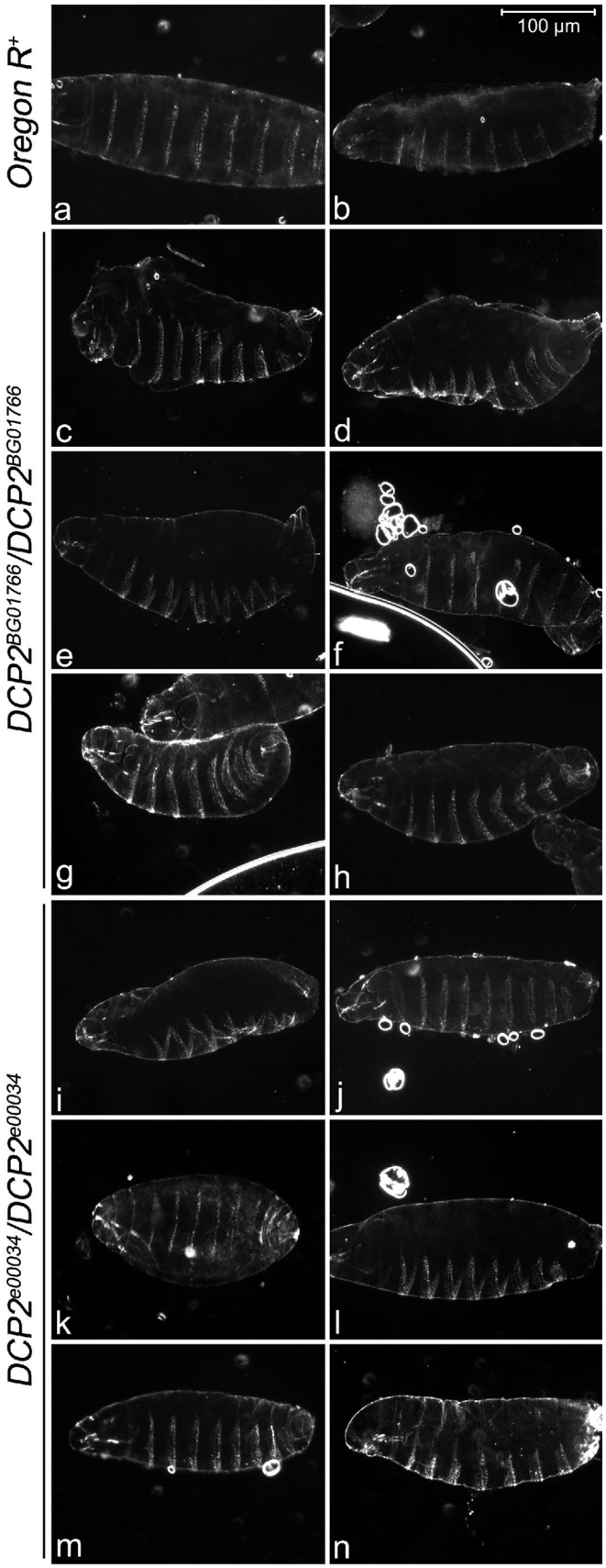

Fig. 6 Dark field photomicrographs of embryonic cuticles of the wild type (**a**, **b**) and *DCP2* loss-of-function homozygotes, *viz*., $DCP2^{BG01766}$ (**c**–**h**) and $DCP2^{e00034}$ (**i**–**n**). Note the altered dimensions and/or morphology and defects in head involution exhibited by the mutants as compared to the wild type. Scale bar (in **b**) shows 100 µm

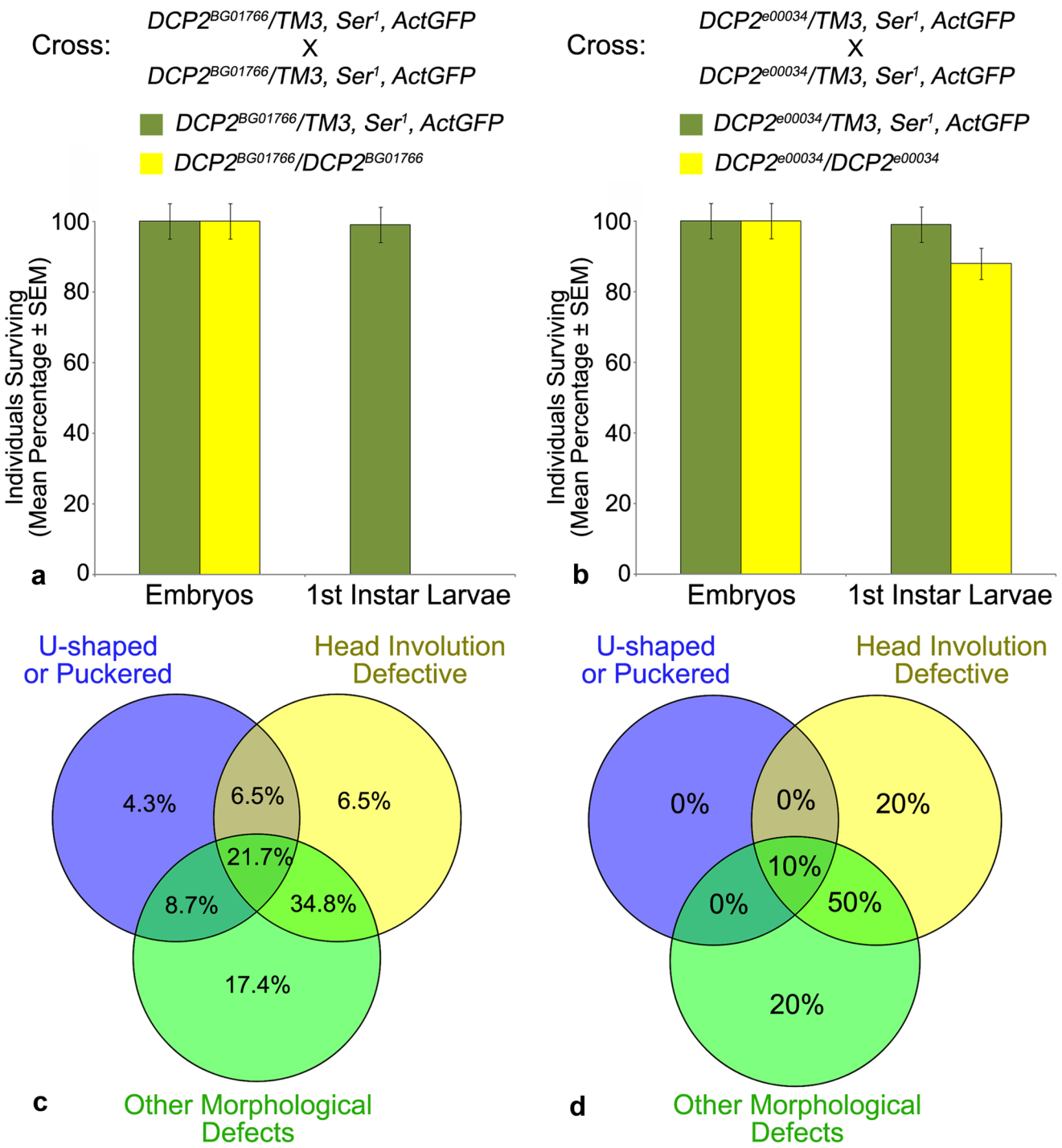

Fig. 7 Embryonic lethality and defects in epithelial morphogenesis in *DCP2* loss-of-function homozygotes. $DCP2^{BG01766}$ homozygotes are 100% embryonic lethal (**a**) and exhibit a broader range of epithelial morphogenesis defects being altered in anterioposterior or dorsoventral dimensions along with puckering and defective head involution (**c**), but $DCP2^{e00034}$ homozygotes show only 12% lethality at the embryonic stage (**b**) and display a milder range of defects with none of them being exclusively u-shaped or puckered (**d**)

neuronal structures expressing FasII, *viz*., the Mushroom Body and the neurons innervating the eye, in the central brain (Fig. 11d–f) and in the dorsolateral and dorsomedial longitudinal tracts in the VNC (Fig. 11g–i), the DL neurons appear to innervate the Ring gland and the aorta. Lateral views of the central brain (Fig. 11d′-f′) and the VNC (Fig. 11g′-i′) show that the DCP2-positive neurons lie below the Fas II immunopositive dorsolateral and dorsomedial

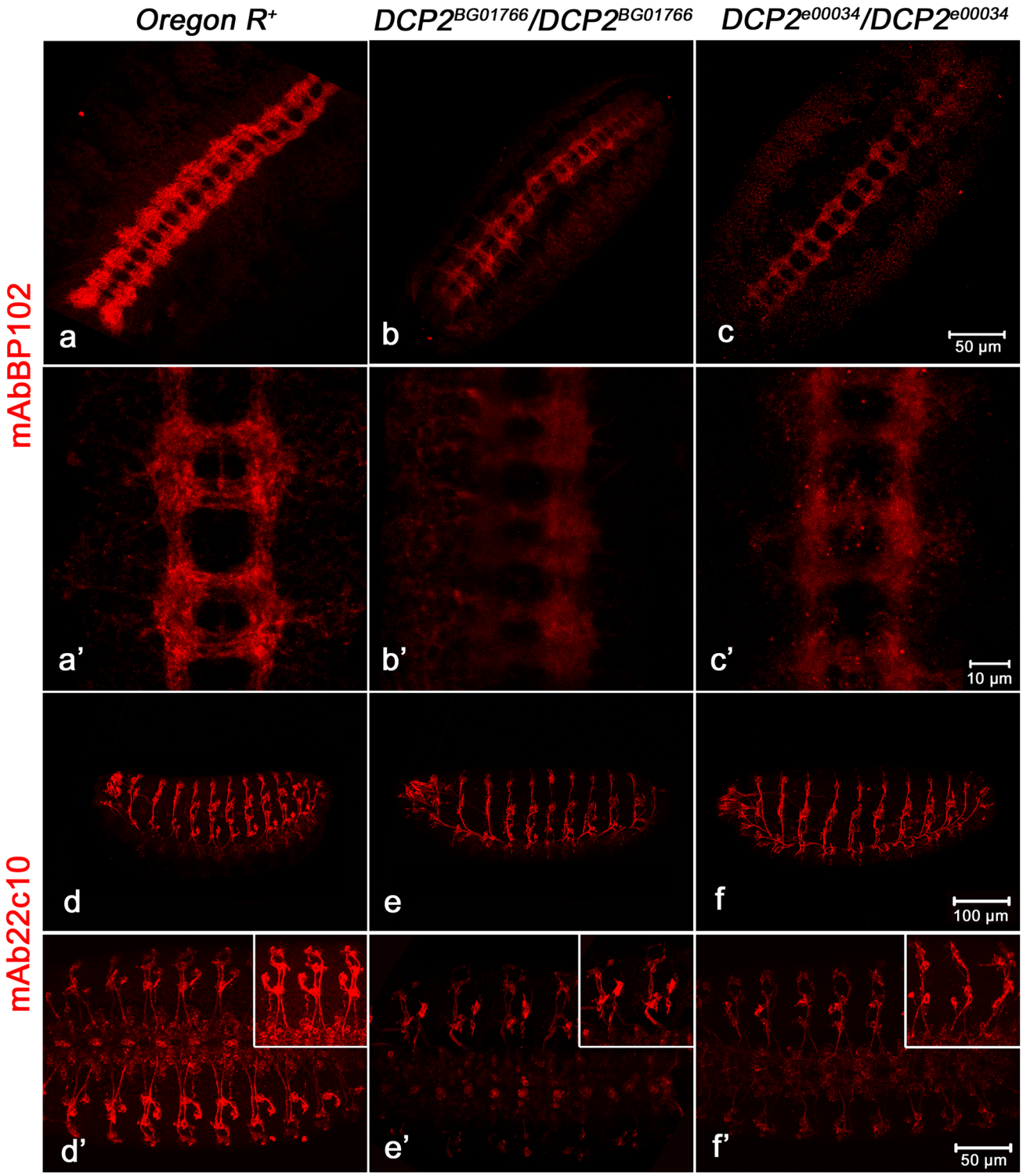

Fig. 8 *DCP2* null homozygotes display defects in CNS and PNS organization. Upper panel: Wild-type embryos, stained with mAbBP102 show regular arrangement of longitudinal connectives and segmental commissures (**a**, **a′**). $DCP2^{BG01766}$ homozygotes showed thinning of longitudinal connectives and compressed segmental commissures (**b**, **b′**), whereas $DCP2^{e00034}$ homozygotes showed thinning of longitudinal connectives and lateral commissures (**c**, **c′**). Lower panel: In the PNS, axons run from the ventral nerve cord to the periphery of the embryos in each hemisegment (**d**, **d′**). A loss of *DCP2* causes misrouting and collapse of fasciculating axons (**e**, **e′**; **f**, **f′**). Scale bars show 50 µm in **a**-**c** and **d'**-**f'**, 10 µm in **a'**-**c'** and 100 µm in **d**-**f**

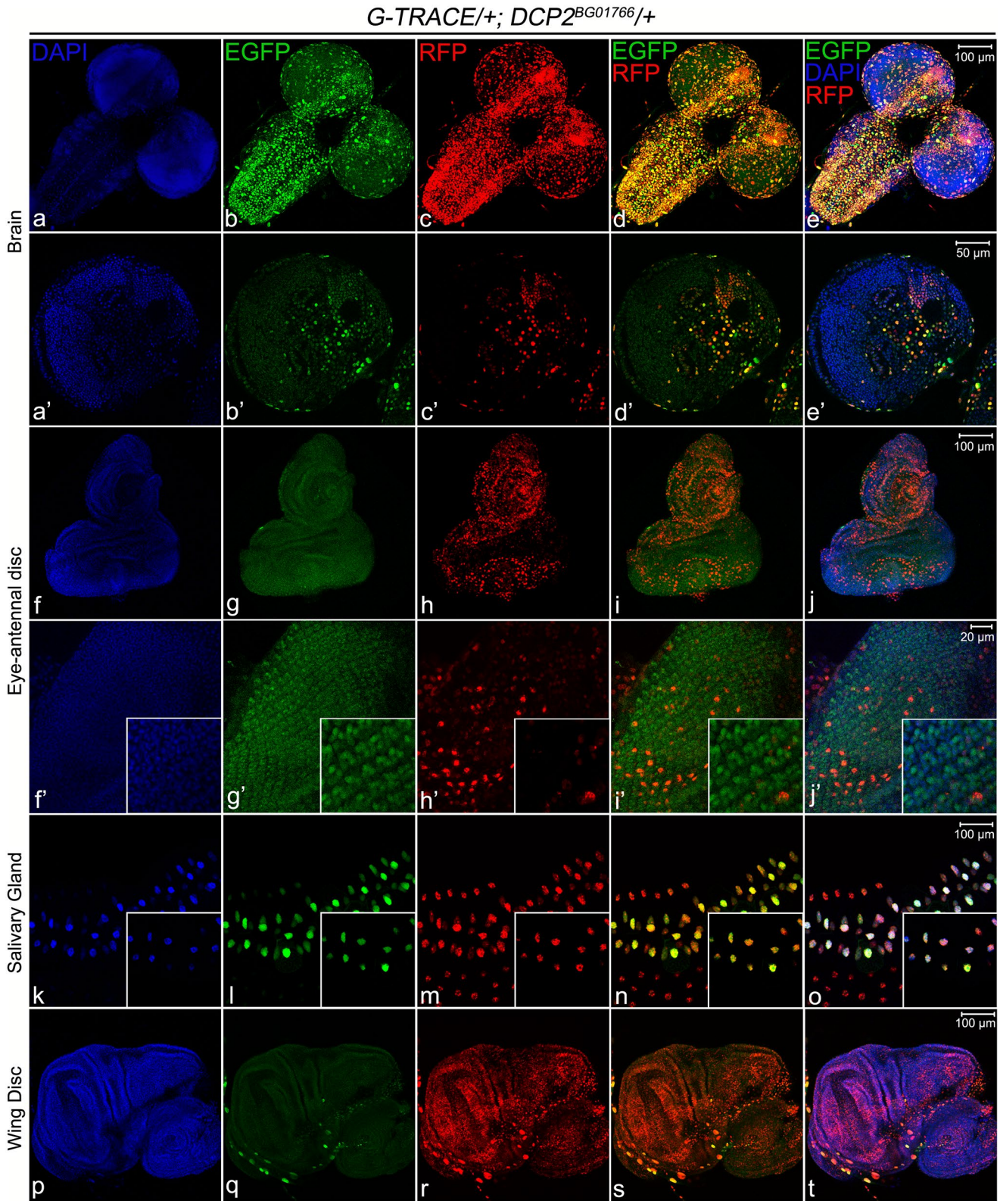

Fig. 9 Lineage-specific (EGFP) and real-time (RFP) expression of *DCP2* in the larval tissues using the GAL4-UAS-based G-TRACE system. Although the ventral ganglion (**b**, **c**) and the antennal disc (**g**, **h**) show significant overlap of the reporters, the central brain (**b′**, **c′**) and the eye-disc (**g′**, **h′**) show heterogeneity of expression. The salivary gland nuclei and the wing disc show strong real-time expression of the *DCP2* promoter along with prior developmental expression. Scale bars show 50 µm in **a′**–**e′**, 20 µm in **f′**–**j′** and 100 µm in rest

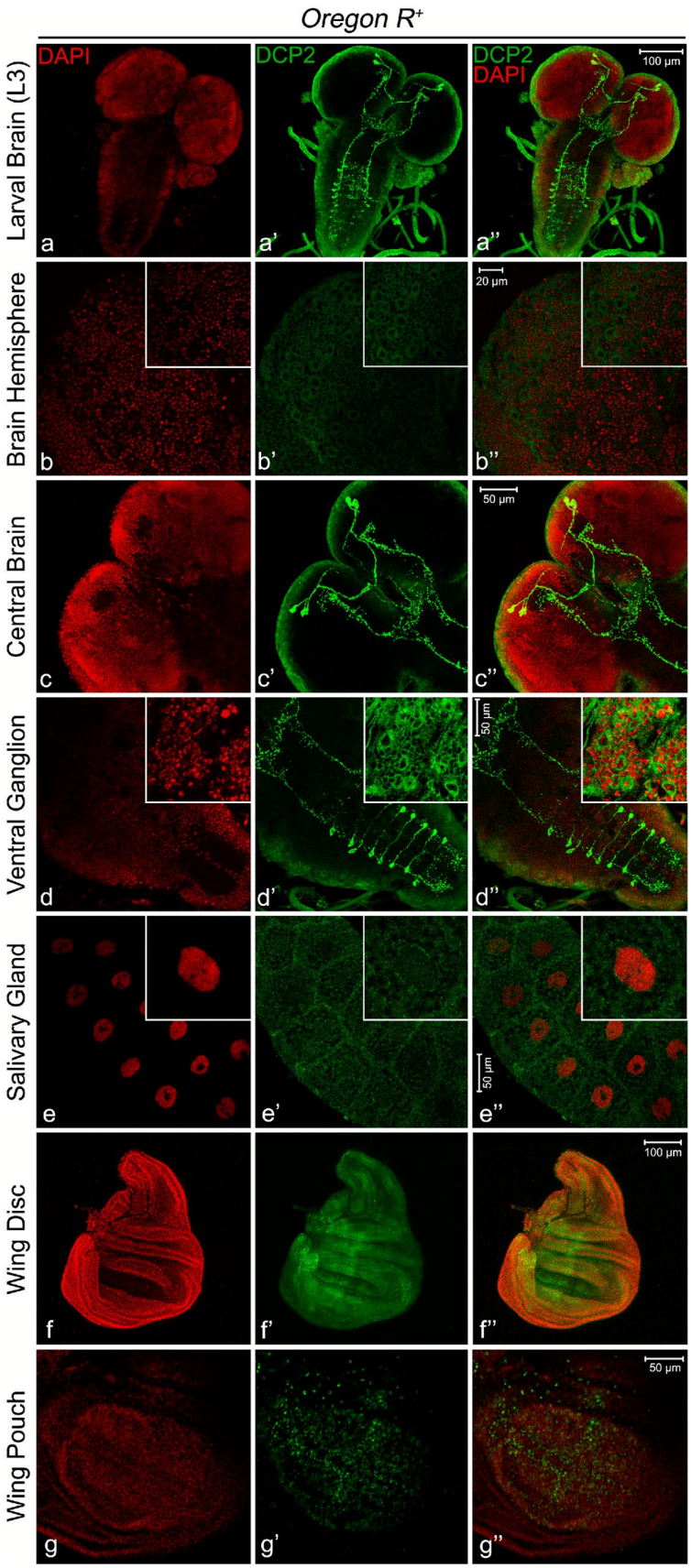

Fig. 10 Confocal projections showing immunolocalisation of DCP2 in the larval tissues. **a**–**a″** (Scale bar shows 100 µm) shows the expression pattern in the larval brain. **b** (Scale bar shows 20 µm), **c**, **d** (Scale bar shows 50 µm) show higher magnifications of the same, wherein we find a ubiquitous cytoplasmic expression of DCP2. Visible in **c′** and **d′** are a subset of neurons which show high expression of DCP2. In the salivary glands (**e**; scale bar shows 50 µm), besides cytoplasmic expression, the vesicles in the cytoplasm appear to be arduously decorated with punctate distribution of DCP2. **f** (scale bar shows 100 µm) shows the pattern of expression of DCP2 in the wing disc. Shown in **g** (scale bar shows 50 µm) is a section of the wing pouch which shows a magnified view wherein DCP2 at the anterioposterior and dorsoventral margins in a cruciform pattern

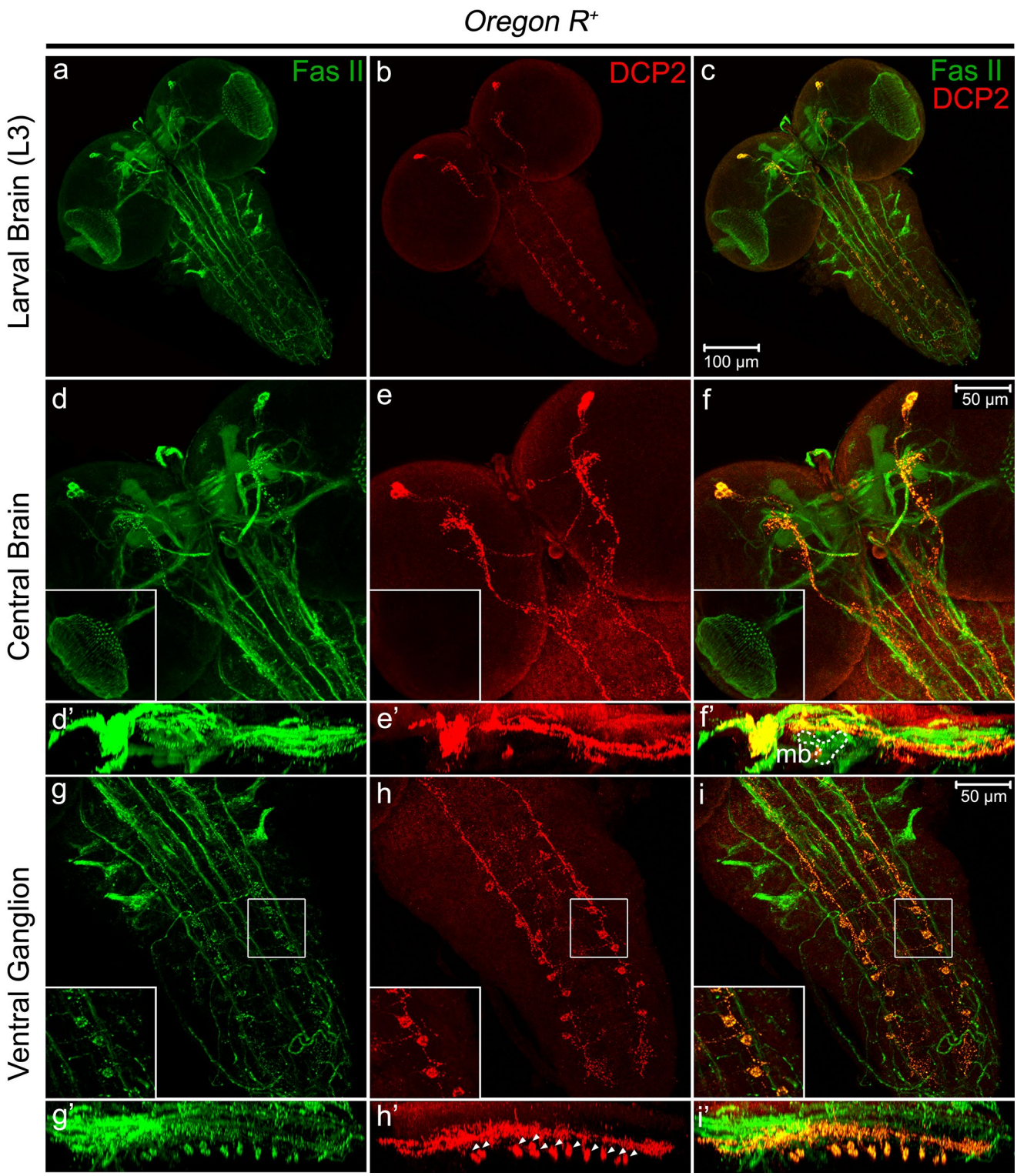

Fig. 11 Mapping of the neuron(s) expressing high titres of DCP2 in the whole mount preparations of the larval brain (**a**–**c**) in the FasII landmark system (Santos et al. 2007). Note the absence of DCP2 in the neurons of the optic lobe (inset **d**–**f**). Z-axis stacks show that the DCP2 positive immunopositive neuronal tracts lie below the FasII immunopositive tracts in the larval ventral ganglion but ascend over the Mushroom Body (mb) in the central brain (**d′**–**f′**). However, a subset of thoracic and abdominal neuromeres co-express FasII and DCP2 (**g**–**i**). Z-axis stacks (**g′**–**i′**) showing lateral view of the larval ventral ganglion depicted in **g**–**i** demonstrate co-expression of FasII and DCP2 in the neuromeres. Scale bars show 100 µm in **a**–**c** and 50 µm in **d**–**i**

longitudinal tracts but ascend above the Mushroom Body (MB) in the central brain.

While DCP2 did not show co-expression with the different neuropeptides *viz*., Crustacean cardioactive peptide (CCAP; Veverytsa and Allan 2012), *Drosophila* insulin-like peptide-2 (Dilp2; Liu et al. 2016), biogenic amines tryptophan hydroxylase (TH; Friggi-Grelin et al. 2003) and dopamine decarboxylase (Ddc; Vomel and Wegener 2008) or the transcription factor Apterous (Ap; Rincon-Limas et al. 1999) (Supplementary Fig. 3), complete colocalization or overlap of expression was observed with the neurons expressing Corazonin (Crz; Lee et al. 2008) (Fig. 12), while only the dorsolateral neurons showed co-expression with short neuropeptide F (sNPF; Nassel et al. 2008)

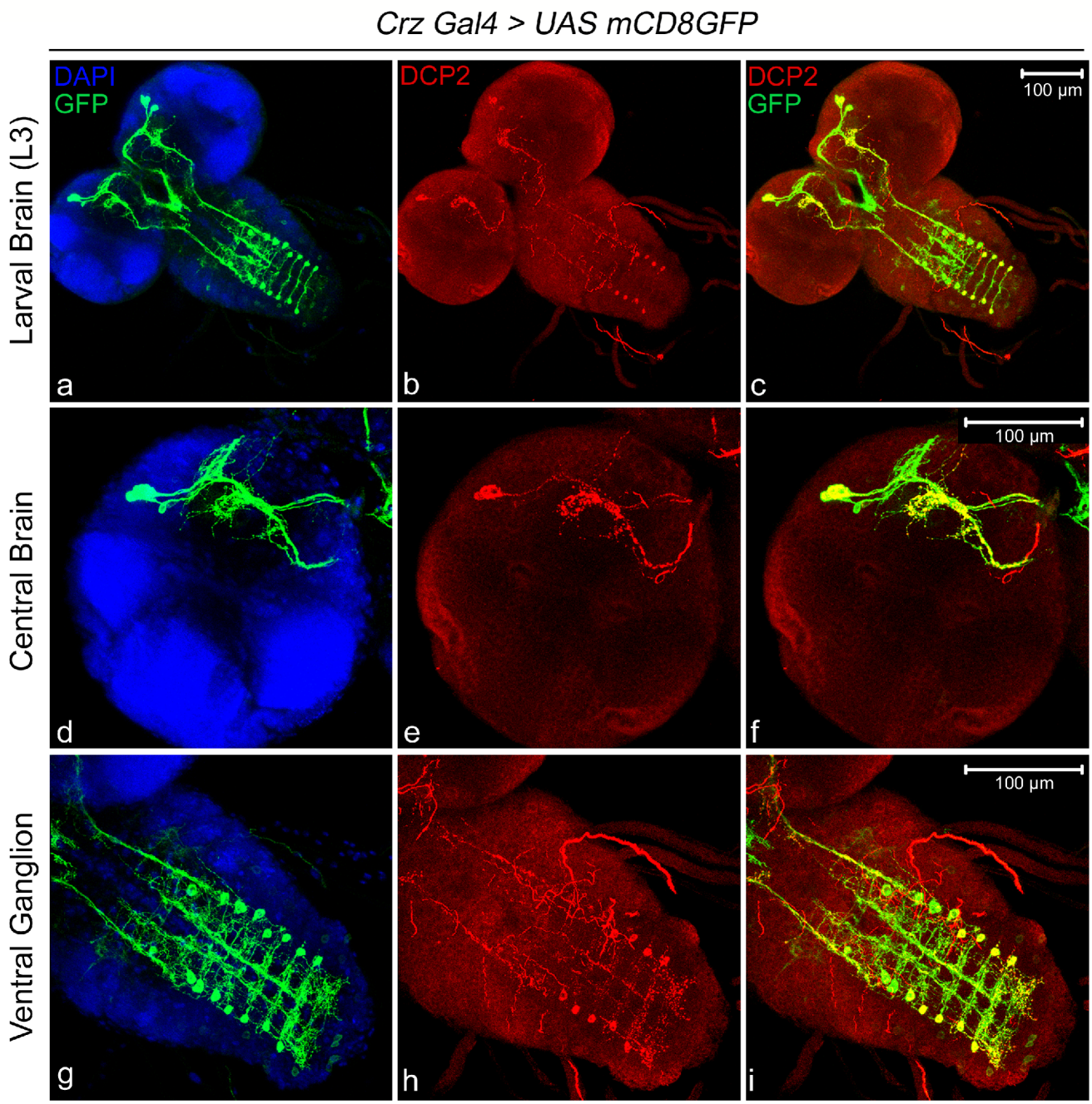

Fig. 12 Mapping of the neuron(s) expressing DCP2 in the whole mount preparations of the larval brain against the Corazonin expressing neurons. **a**–**c** shows the expression pattern of DCP2 and Corazonin neurons in the larval brain. **d**–**f** and **g**–**i** show magnified view of the central brain and the ventral ganglion respectively, where complete colocalization of DCP2 and Corazonin is visible. Scale bars show 100 µm

(Supplementary Fig. 4). Corazonin neurons constitute three neuronal subsets, *viz*., the dorsolateral (DL) and dorsomedial Crz neurons (DM), and the Crz neurons in the ventral nerve cord (vCrz) (Lee et al. 2008) are essential for combating stress (Zhao et al. 2010) and co-express the transcription factor Apontic, which is necessary and sufficient to mediate sensitivity to ethanol (McClure 2013).

Knockdown of *DCP2* in the Corazonin neurons reduces sensitivity to Ethanol

We further asked whether *DCP2* function in the Corazonin neurons is required for their activity. When *DCP2* was knocked down in these neurons specifically, it did not affect the morphology, path finding or architecture of the Crz neurons in the larval brain (Supplementary Fig. 5) but delayed and/or reduced the sedation sensitivity to ethanol in the adult flies. The time to 50% sedation (ST50) was calculated to be ~ 8.5 min for the control flies ($N = 200$), while the *DCP2* knocked-down flies showed an ST50 of ~ 13.5 min ($N = 200$). While the control flies are sedated completely in ~ 12 min, the *DCP2* hypomorphs are active till ~ 19 min (Fig. 13a, b). This demonstrates the reduced sensitivity of the *Crz GAL4 > UAS DCP2*^{RNAi} knocked-down flies to ethanol.

Following sedation, the DCP2 hypomorphs showed early onset of recovery (~ 30 min) as against the control flies, which started showing activity/onset of recovery after ~ 110 min. While the control flies started assuming normal standing posture in ~ 2 h, the *DCP2* knocked-down flies showed significant early recovery, with ~ 80% of the flies recovering by 3 h as against ~ 40% recovery exhibited by the control flies in the same time (Fig. 13c, d). Also, sedation-induced death was higher in the control group as compared to the *DCP2* hypomorphs. During sedation and recovery phases, no sex-specific differences were observed in flies of either genotype. These results suggest that DCP2-mediated protein turnover is essential in the Crz neurons for regulation of ethanol-related behaviour and ethanol metabolism.

The Crz neurons require the transcription factor Dimmed and its target enzyme, peptidylglycine-alpha-hydroxylating monooxygenase (PHM) (Park et al. 2008), for synthesis of Corazonin while the transcription factor Apontic (Apt) is necessary and sufficient for regulating the activity of the Crz neurons and/or release of Corazonin during ethanol exposure (McClure 2013). The delay in sedatory behaviour during ethanol exposure and the quick recovery from sedation demonstrate perturbed corazonin signalling following knockdown of *DCP2* in the Crz neurons, although the mechanism behind such altered physiology remains unknown.

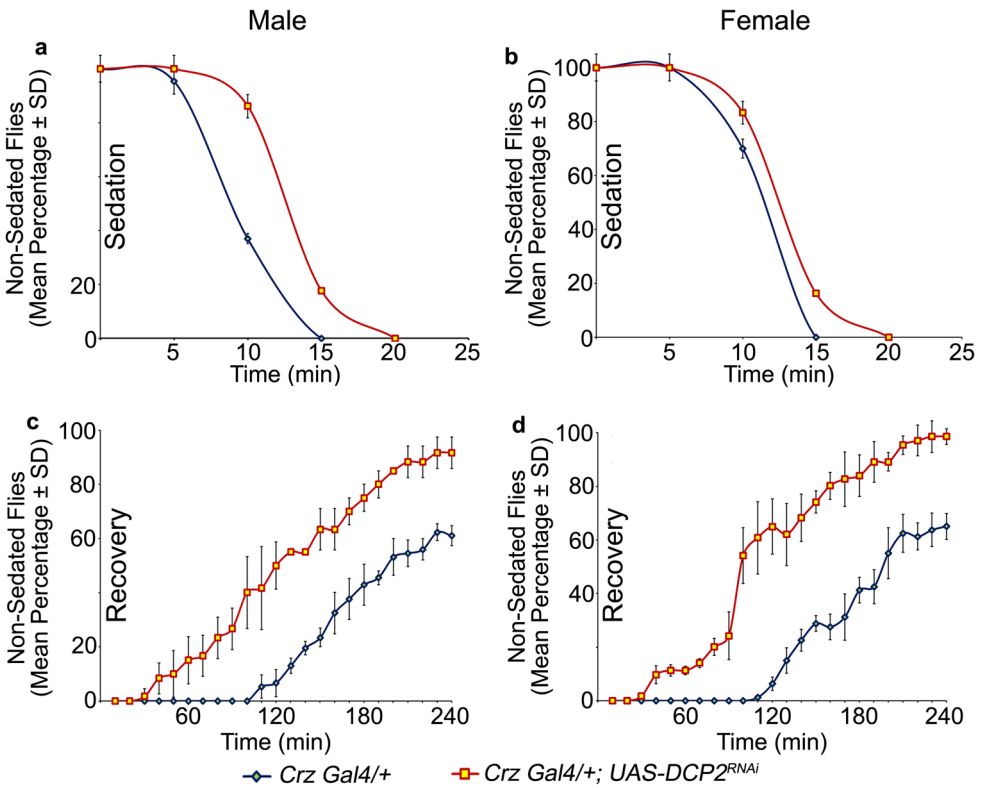

Fig. 13 Graphs showing the response to ethanol-induced sedation (**a**, **b**) in the control (*Crz-Gal4/+*; blue lines) or *DCP2* knocked down (*Crz-Gal4/+*; *UAS-DCP2*^{RNAi}*/+*) flies (red lines) and recovery from the same (**c**, **d**). The knocked-down flies (both male and female) show reduced sensitivity to ethanol vapours as is visible from their delayed sedation behaviour (**a**, **b**) or enhanced recovery from sedation (**c**, **d**)

Summary and conclusion

Analysis and identification of the expression patterns of genes and/or proteins in model organisms across the evolutionary tree are important for understanding the spectral paradigm of gene function. The extent to which a gene and its expressome are conserved across diverse organisms indicates the precision of its function across phyla. mRNA decapping proteins are present in all metazoans and serve to initiate the decay of mRNA and are therefore important for regulation of gene expression *vis-à-vis* cellular physiology. The patterns of expression and paradigm range of physiological aberrations following the ablation or knockdown of *DCP2* is indicative of the fundamental regulatory role played by it during development and bring to light the hitherto undiscovered plausible novel functions of DCP2. It is yet unknown as to whether its function in the modulation of developmental events is *via* its primary function of mRNA decapping *per se* or is a manifestation of moonlighting properties (Mani et al. 2014). Summarizing the present observations, our findings demonstrate that *DCP2* plays a major modulatory function in developmental gene expression and is essential for maintenance of organismal physiology at all stages of development.

Supplementary information The online version contains supplementary material available at https://doi.org/10.1007/s00441-021-03503-x.

Acknowledgements The authors acknowledge the fly community for generously providing the fly stocks. We thank Prof. B. J. Rao, TIFR, Mumbai for providing the *TRE-JNK/CyO* stock; Prof. Gaiti Hasan, NCBS, Bangalore, for providing the *sNPF-GAL4*, *Dilp2-GAL4* and *Crz-GAL4/CyO* stocks and Prof. Utpal Banerjee, UCLA, for providing the *G-TRACE/CyO* flies. We duly acknowledge the National Facility for Laser Scanning Confocal Microscopy, Department of Zoology, Banaras Hindu University. The equipment facility supported by UGC-CAS, DST-FIST, and IoE to Department of Zoology are duly acknowledged. We sincerely acknowledgeNabarun Nandy for the assistance and valuable discussions. We sincerely thank Department of Science and Technology (DST) for providing fellowship to RK and support to JKR.

Author contribution RK: conceptualization, resources, methodology, investigation, data curation, formal analysis and interpretation, writing the manuscript. JKR: supervision, resources, writing the manuscript.

Funding Financial support received from Department of Science and Technology, New Delhi in the form of fellowship to RK is acknowledged.

Declarations

Ethics approval All studies were performed as per ethical guidelines. All applicable international, national, and/or institutional guidelines for the care and use of flies were followed.

Conflict of interest The authors declare no competing interests.

References

Bahri S, Wang S, Conder R, Choy J, Vlachos S, Dong K, Merino C, Sigrist S, Molnar C, Yang X, Manser E (2010) The leading edge during dorsal closure as a model for epithelial plasticity: Pak is required for recruitment of the Scribble complex and septate junction formation. Development 137:2023–2032

Banerjee A, Roy JK (2017) Dicer-1 regulates proliferative potential of *Drosophila* larval neural stem cells through bantam miRNA based down-regulation of the G1/S inhibitor Dacapo. Dev Bio 423:57–65

Ding B (2015) Gene expression in maturing neurons: regulatory mechanisms and related neurodevelopmental disorders. Acta Physiol Sinica 67:113–133

Bhuin T, Roy JK (2009) Rab11 is required for embryonic nervous system development in *Drosophila*. Cell Tissue Res 335:349–356

Brand AH, Perrimon N (1993) Targeted gene expression as a means of altering cell fates and generating dominant phenotypes. Development 118:401–415

Chatterjee N, Bohmann D (2012) A versatile ΦC31 based reporter system for measuring AP-1 and Nrf2 signaling in *Drosophila* and in tissue culture. PloS One 7: e34063

Coller J, Parker R (2004) Eukaryotic mRNA decapping. Ann Rev. Biochem 73:861–890

Dreos R, Ambrosini G, Groux R, Cavin Périer R, Bucher P (2017) The eukaryotic promoter database in its 30th year: focus on non-vertebrate organisms. Nucl Acid Res 45:D51–D55

Dreos R, Ambrosini G, Périer RC, Bucher P (2014) The Eukaryotic Promoter Database: expansion of EPDnew and new promoter analysis tools. Nucl Acids Res 43:D92–D96

Drysdale R, FlyBase Consortium (2008) FlyBase. In: *Drosophila* pp. 45-59. Humana Press

Evans CJ, Olson JM, Ngo KT, Kim E, Lee NE, Kuoy E, Patananan AN, Sitz D, Tran P, Do MT, Yackle K (2009) G-TRACE: rapid Gal4-based cell lineage analysis in *Drosophila*. Nat Methods 6:603

Friggi-Grelin F, Coulom H, Meller M, Gomez D, Hirsh J, Birman S (2003) Targeted gene expression in *Drosophila* dopaminergic cells using regulatory sequences from tyrosine hydroxylase. J Neurobiol 54:618–627

Fujita SC, Zipursky SL, Benzer S, Ferrus A, Shotwell SL (1982) Monoclonal antibodies against the *Drosophila* nervous system. Proc Natl Acad Sci 79:7929–7933

Ghosh S, Jacobson A (2010) RNA decay modulates gene expression and controls its fidelity. Wiley Interdisciplinary Reviews: RNA 1:351–361

Goeres DC, Van Norman JM, Zhang W, Fauver NA, Spencer ML, Sieburth LE (2007) Components of the Arabidopsis mRNA decapping complex are required for early seedling development. Plant Cell 19:1549–1564

Hartenstein V (1993) *Atlas of Drosophila development* 328. Cold Spring Harbor Laboratory Press

Hummel T, Krukkert K, Roos J, Davis G, Klämbt C (2000) *Drosophila* Futsch/22C10 is a MAP1B-like protein required for dendritic and axonal development. Neuron 26:357–370

Hummel T, Schimmelpfeng K, Klämbt, C (1999) Commissure Formation in the Embryonic CNS of *Drosophila*: I. Identification of the Required Gene Functions. Developmental biology 209: 381-398.

Jacinto A, Woolner S, Martin P (2002) Dynamic analysis of dorsal closure in *Drosophila*: from Genetics to Cell Biology. Dev Cell 3:9–19

Karkali K, Saunders TE, Vernon SW, Baines RA, Panayotou G, Martin-Blanco E (2020) JNK signaling in pioneer neurons directs the

architectural organization of the CNS and coordinates the motor activity of the *Drosophila* embryo. BioRxiv: 092486
Kushnir T, Mezuman S, Bar-Cohen S, Lange R, Paroush ZE, Helman A (2017) Novel interplay between JNK and Egfr signaling in *Drosophila* dorsal closure. PLoS Genet 13: e1006860
Lada K, Gorfinkiel N, Arias AM (2012) Interactions between the amnioserosa and the epidermis revealed by the function of the u-shaped gene. Biology Open 1:353–361
Lakhotia SC, Mallik M, Singh AK, Ray M (2012) The large noncoding hsrω-n transcripts are essential for thermotolerance and remobilization of hnRNPs, HP1 and RNA polymerase II during recovery from heat shock in *Drosophila*. Chromosoma 12:49–70
Lall S, Piano F, Davis RE (2005) *Caenorhabditis elegans* decapping proteins: localization and functional analysis of Dcp1, Dcp2, and DcpS during embryogenesis. Mol Biol Cell 16:5880–5890
Lee G, Kim KM, Kikuno K, Wang Z, Choi YJ, Park JH (2008) Developmental regulation and functions of the expression of the neuropeptide corazonin in *Drosophila* melanogaster. Cell Tissue Res 331:659–673
Lin MD, Fan SJ, Hsu WS, Chou TB (2006) *Drosophila* decapping protein 1, dDcp1, is a component of the oskar mRNP complex and directs its posterior localization in the oocyte. Dev Cell 10:601–613
Lin MD, Jiao X, Grima D, Newbury SF, Kiledjian M, Chou TB (2008) *Drosophila* processing bodies in oogenesis. Dev Bio 322:276–288
Liu Y, Liao S, Veenstra JA, Nässel DR (2016) *Drosophila* insulin-like peptide 1 (DILP1) is transiently expressed during non-feeding stages and reproductive dormancy. Sci Rep 6:26620
Lukacsovich T, Asztalos Z, Awano W, Baba K, Kondo S, Niwa S, Yamamoto D (2001) Dual-tagging gene trap of novel genes in *Drosophila melanogaster*. Genetics 157:727–742
Mani M, Chen C, Amblee V, Liu H, Mathur T, Zwicke G, Zabad S, Patel B, Thakkar J, Jeffery CJ (2014) MoonProt: a database for proteins that are known to moonlight. Nucl Acid Res 43:D277–D282
Martinez Arias A (1993) Development and patterning of the larval epidermis of *Drosophila*. In: The Development of *Drosophila melanogaster* I, pp. 517–608, CSHL Press
McClure KD, Heberlein U (2013) A small group of neurosecretory cells expressing the transcriptional regulator apontic and the neuropeptide corazonin mediate ethanol sedation in *Drosophila*. J Neurosci 33:4044–4054
Nandy N, Roy JK (2020) Rab11 is essential for lgl mediated JNK–Dpp signaling in dorsal closure and epithelial morphogenesis in *Drosophila*. Dev Bio 464:188–201
Narasimha M, Brown NH (2006) Confocal microscopy of *Drosophila* embryos. In: Cell Biology-A Laboratory Handbook (ed.) JE Celis, pp77–86. Academic Press
Nässel DR, Enell LE, Santos JG, Wegener C, Johard HA (2008) A large population of diverse neurons in the *Drosophila* central nervous system expresses short neuropeptide F, suggesting multiple distributed peptide functions. BMC Neurosci 9:90
Neumann CJ, Cohen SM (1997) Long-range action of Wingless organizes the dorsal-ventral axis of the *Drosophila* wing. Development 124:871–880
Noselli S, Agnès F (1999) Roles of the JNK signaling pathway in *Drosophila* morphogenesis. Curr Opin Genet Dev 9:466–472
Noselli S (1998) JNK signaling and morphogenesis in *Drosophila*. Trends Genet 14:33–38
Park D, Veenstra JA, Park JH, Taghert PH (2008) Mapping peptidergic cells in *Drosophila*: where DIMM fits in. PloS One 3:e1896
Rämet M, Lanot R, Zachary D, Manfruelli P (2002) JNK signaling pathway is required for efficient wound healing in *Drosophila*. Dev Bio 241:145–156
Rehwinkel JAN, Behm-Ansmant I, Gatfield D, Izaurralde E (2005) A crucial role for GW182 and the DCP1: DCP2 decapping complex in miRNA-mediated gene silencing. RNA 11:1640–1647
Ren J, Sun J, Zhang Y, Liu T, Ren Q, Li Y, Guo A (2012) Down-regulation of decapping protein 2 mediates chronic nicotine exposure-induced locomotor hyperactivity in *Drosophila*. PloS One 7:e52521
Rincón-Limas DE, Lu CH, Canal I, Calleja M, Rodríguez-Esteban C, Izpisúa-Belmonte JC, Botas J (1999) Conservation of the expression and function of apterous orthologs in *Drosophila* and mammals. Proc Natl Acad Sci 96:2165–2170
Santos JG, Vömel M, Struck R, Homberg U, Nässel DR, Wegener C (2007) Neuroarchitecture of peptidergic systems in the larval ventral ganglion of *Drosophila melanogaster*. PLoS One 2:e695
Sasikumar S, Roy JK (2009) Developmental expression of Rab11, a small GTP-binding protein in *Drosophila* epithelia. Genesis 47:32–39
Seeger M, Tear G, Ferres-Marco D, Goodman CS (1993) Mutations affecting growth cone guidance in *Drosophila*: genes necessary for guidance toward or away from the midline. Neuron 10:409–426
Sha K, Choi SH, Im J, Lee GG, Loeffler F, Park JH (2014) Regulation of ethanol-related behavior and ethanol metabolism by the Corazonin neurons and Corazonin receptor in *Drosophila melanogaster*. PLoS One 9:e87062
Shklover J, Mishnaevski K, Levy-Adam F, Kurant E (2015) JNK pathway activation is able to synchronize neuronal death and glial phagocytosis in *Drosophila*. Cell Death Dis 6:e1649
Stronach B, Perrimon N (2002) Activation of the JNK pathway during dorsal closure in *Drosophila* requires the mixed lineage kinase, slipper. Genes Dev 16:377–387
Veverytsa L, Allan DW (2012) Temporally tuned neuronal differentiation supports the functional remodeling of a neuronal network in *Drosophila*. Proc Natl Acad of Sci 109:E748–E756
Vömel M, Wegener C (2008) Neuroarchitecture of aminergic systems in the larval ventral ganglion of *Drosophila melanogaster*. PLoS One 3:e1848
Wieschaus E, Nüsslein-Volhard C (1986) *Drosophila*: a practical approach. IRL Press, Oxford, England, p 200
Xu J, Yang JY, Niu QW, Chua NH (2006) *Arabidopsis* DCP2, DCP1 and VARICOSE form a decapping complex required for postembryonic development. Plant Cell 18:3386–3398
Yao T, Ndoja A (2012) Regulation of gene expression by the ubiquitin-proteasome system. Seminars in Cell Dev Bio 23:523–529
Zecca M, Basler K, Struhl G (1995) Sequential organizing activities of engrailed, hedgehog and decapentaplegic in the *Drosophila* wing. Development 121:2265–2278
Zhao Y, Bretz CA, Hawksworth SA, Hirsh J, Johnson EC (2010) Corazonin neurons function in sexually dimorphic circuitry that shape behavioral responses to stress in *Drosophila*. PLoS One 5:e9141